論文 96-21-4-6

Determination of Threshold Values for Color Image Segmentation

Byung-Uk Lee* *Regular Member*

색도 영상분할을 위한 문턱치 결정방법

正會員 이 병 욱*

ABSTRACT

This paper investigates a method for determining a threshold value based on the probability distribution function for color image segmentation. Principal components of normalized color is analyzed and found that there are effective color transforms for outdoor scenes. We explain the functional relationship of the threshold and the probability of a region detection, assuming bivariate Gaussian probability density function. Experimental results show that the probability of detection is proportional to the segmented area.

요 약

색도 영상 분할에서의 문턱치를 결정할 때에, 색도 신호의 확률분포함수 특성을 이용하였다. 정규화된 색상신호의 principal component를 분석하였고 자연영상에 적합한 변환 축이 있음을 밝혔다. 이차원 가우스 분포를 사용할 경우에, 문턱치와 영역 검출 확률과의 관계를 보였다. 영역 검출 확률과 분할된 영역의 면적이 비례관계에 있음을 실험결과에서 볼 수 있었다.

I. Introduction

In many computer vision systems, segmentation of an image is an important first step to image understanding. Digital images are composed of pixels, and the objective of segmentation is to aggregate pixels with homogeneous properties: brightness, color, texture or depth. The outcome of the segmentation is applied to the higher level processing, such as recognition of a target or an obstacle. Also a region can be defined from closed boundaries, which result from abrupt changes in image intensity, surface orientation or depth. Finding discontinuity is a dual problem of a region based segmentation method.

Color has been widely employed in segmenting outdoor scenes [1][2], and it is a reliable feature in segmenting road from natural scenes for autonomous land vehicle applications [3][4]. Gray scale images are

*이화여자대학교 전자공학과
Ewha Womans University
論文番號:96031-0129
接受日字:1996年 1月 29日

influenced by lighting conditions, surface orientation and reflectance of the object, and it is not possible to identify each component from the intensity without additional information or assumptions. However, color constancy is an interesting and useful function of human visual perception which recovers surface spectral reflectance independent of surrounding illumination [5][6]. Color image segmentation is more reliable, since we can reduce the effect of object surface orientation or lighting condition.

Most of the color image segmentation schemes apply thresholding on a one dimensional histogram [1] [2], which becomes a rectangular boundary on the two dimensional color space. Uchiyama and Arbib employed the Vornoi tessellation as in vector quantization [9]. We adopt bivariate Gaussian distribution model for the probability distribution function of the pixels on the color space. Then the decision boundary becomes an ellipse.

In many cases human intervention is required in deciding the threshold value. In this paper we will show the relationship of the threshold level and the probability distribution of the color histogram.

Ⅱ. Color Coordinates

Basic understanding of color has been accomplished by many researchers. Wandell showed a linear model for analysis and synthesis of color images, which is a result of surface spectral reflectance and the ambient light spectral power [7].

Our color segmentation method is based on color histogram. It is interesting to note that color indexing has been popular recently, which compares color histograms. It is relatively independent of view point, scale or occlusion [8]. The idea of color indexing has been extended to local color histogram [11] and combined with color constancy algorithm [12].

There are many color coordinate systems [7][13], and the color coordinates play an important role in segmentation [2][14][15]. Ohta et al. found that I1 = (R + G + B)/3, I2 = (R − B)/2, and I3 = (2G − R − B)/4 are effective features, which are good approximations of Karhunen-Loeve (KL) transform coordinates [2]. We have employed normalized color, where red (R), green (G), and blue (B) color components are divided by intensity, $I1 = (R + G + B)/3$, to reduce the influence of the surface orientation or illumination [18].

$$I1 = (R + G + B)/3$$
$$r = R/I1$$
$$g = G/I1$$
$$b = B/I1$$

For a matte surface, we can use the Lambertian reflectance model, where the image intensity is proportional to the product of incident light, surface reflectance and the cosine of the incidence angle.

$$R = k_R R_i \rho_R \cos\theta$$
$$G = k_G G_i \rho_G \cos\theta$$
$$B = k_B B_i \rho_B \cos\theta$$

, where k is the constant which depends on the aperture and focal length of the camera lens, optical color filter, etc. Ri, Gi, and Bi are red, green, and blue components of the illumination, ρ is the matte surface reflectance, and θ is the angle of incidence. The normalized color is independent of the orientation of the surface as shown in the following equation.

$$r = R/(R+G+B) = k_R R_i \rho_R/(k_R R_i \rho_R + k_G G_i \rho_G + k_B B_i \rho_B)$$
$$g = G/(R+G+B) = k_G G_i \rho_G/(k_R R_i \rho_R + k_G G_i \rho_G + k_B B_i \rho_B)$$
$$b = B/(R+G+B) = k_B B_i \rho_B/(k_R R_i \rho_R + k_G G_i \rho_G + k_B B_i \rho_B)$$

If the illumination changes by a scale factor preserving the shape of the spectrum, it does not affect the normalized color image. Therefore if the spectrum of the illumination is constant over the Lambertian surface objects, the normalized color is proportional to the surface reflectance. However we need elaborate algorithms to achieve color constancy, to consider the

Fig. 1 A road image.

effect of illumination, specular reflectance components and the nonlinearity of the image sensor response.

KL coordinates on the normalized color components are determined from a test image [Fig. 1]. The covariance matrix Σ is defined as

$$\Sigma = \frac{1}{MN} \sum_{j=1}^{M} \sum_{k=1}^{N} (r_{jk}-\bar{r}, g_{jk}-\bar{g}, b_{jk}-\bar{b})^T (r_{jk}-\bar{r}, g_{jk}-\bar{g}, b_{jk}-\bar{b})$$

, where $(\bar{r}, \bar{g}, \bar{b}) = \frac{1}{MN} \sum_{j=1}^{M} \sum_{k=1}^{N} (r_{jk}, g_{jk}, b_{jk})$ is the mean of the normalized color components. (r_{jk}, g_{jk}, b_{jk}) is the normalized color vector of the pixel at position (j, k) of the image. M and N are the width and the height of the image respectively. The covariance matrix of the Fig. 1 is as follows.

$$\Sigma = \begin{bmatrix} -0.02596 & -0.02489 & -0.00107 \\ -0.02489 & 0.05395 & -0.02906 \\ -0.00107 & -0.02906 & 0.03013 \end{bmatrix}$$

Note that Σ has rank 2, since the color components has been normalized, i.e. r + g + b = 3. After singular value decomposition we obtain two eigen vectors, e_1 and e_2.

$e_1 = -0.358r + 0.815g - 0.456b$
$e_2 = 0.734r - 0.0564g - 0.677b$

with eigen values 0.0812 and 0.0289 respectively. This shows that e_1 has more discriminating power than e_2, since it has the larger eigen value. We can see that e_1 is almost parallel to I3/I1 and e_2 to I2/I1. We have done experiments with other images from natural scenes, and obtained similar results. For simplicity we have chosen color coordinates c1 and c2 following the normalized version of Ohta et al.'s I3 and I2, respectively. Note that cross product of c_1 and c_2 is in the direction of r + g + b vector.

$$i_2 = I2/I1 = (R-B)/2I1 \qquad = (r-b)/2$$
$$i_3 = I3/I1 = (2G-R-B)/4I1 = (2g-r-b)/4$$

$$c_1 = (2g-r-b)/\sqrt{6}$$
$$c_2 = (r-b)/\sqrt{2}$$

Ⅲ. Threshold Value

Usually selection of a threshold value is an interactive process, to reduce the probability of error which is the sum of false positive and false negative. Selection of the threshold value has been investigated by many researchers [10]. We present a method of deciding threshold level based on probability density function (p.d.f.).

We can see that each region has a well separated multimodal distribution as shown in the two dimensional histogram [Fig. 2]. Let $g(c_1, c_2)$ represent the multimodal p.d.f. of the pixels on the KL color image space (c_1, c_2), then it can be represented as the sum of p.d.f.'s of each region, $f_i(c_1, c_2)$.

$$g(c_1, c_2) = \sum_{i=1}^{m} p_i f_i(c_1, c_2)$$

with $\sum_{c_1, c_2} f_i(c_1, c_2) = 1$ and $\sum_{i=1}^{m} p_i = 1$, where, $f_i(c_1, c_2)$ is the p.d.f. the i-th region, m is the number of regions, and p_i is a priori probability of the region which is proportional to the area.

We assume Gaussian probability distribution function for each region, and the hypothesis is verified using a statistical testing method as shown in [17]. The bivariate normal distribution function of the i-th region is

$$f_i(c_1, c_2) = \frac{1}{2\pi\sigma_{i1}\sigma_{i2}\sqrt{1-\rho_i^2}} \quad e^{-U_i(c_1, c_2)/2}$$

where,

$$U_i(c_1, c_2) = \frac{1}{1-\rho_i^2}\left[\frac{(c_1-\mu_{i1})^2}{\sigma_{i1}^2} - 2\rho_i\left(\frac{c_1-\mu_{i1}}{\sigma_{i1}}\right)\left(\frac{c_2-\mu_{i2}}{\sigma_{i2}}\right) + \frac{(c_2-\mu_{i2})^2}{\sigma_{i2}^2}\right]$$

, ρ_i is the correlation coefficient, μ_{i1} and μ_{i2} are the means and σ_{i1} and σ_{i2} are the standard deviations of c_1 and c_2 respectively. We obtained the bivariate normal distribution parameters of each region from the two dimensional histogram on the color space. We know that the correlation coefficient ρ_i is very small after KL transformation. It is known that $U_i(c_1, c_2)$ follows χ^2 distribution with 2 degrees of freedom [16]. From numerical calculation of χ^2 distribution [17], we can obtain the following table, which shows the relationship of the threshold value u and the probability of detection $\text{Prob}(U_i \leq u)$.

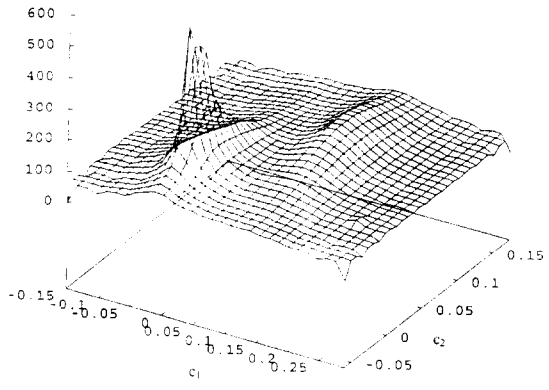

Fig. 2 Two dimensional histogram of the test image in c_1 and c_2 coordinates.

u	$\text{Prob}(U_i \leq u)$
0.211	0.1
0.446	0.2
0.713	0.3
1.02	0.4
1.39	0.5
1.83	0.6
2.41	0.7
3.22	0.8
4.61	0.9
5.99	0.95
7.38	0.975

For a given threshold value of u, the probability of false negative is $1-\text{Prob}(U_i \leq u)$, while the false positive probability depends on the neighboring distributions. From the table, we can observe that employing a threshold value larger than 6 does increase the possibility of false positive without much gain in the probability of detection.

The mean and standard deviation of the road segment were calculated from a sample region, and the thresholded image for each probability is shown in Fig. 3, which shows the segmentation results we have expected. The segmentation from color components without normalization is shown in Fig. 4, where we can notice that other areas are also included in the road region which results in higher false positive error.

We can observe that the area of the segmented region is proportional to the probability of detection as shown in Fig. 5.

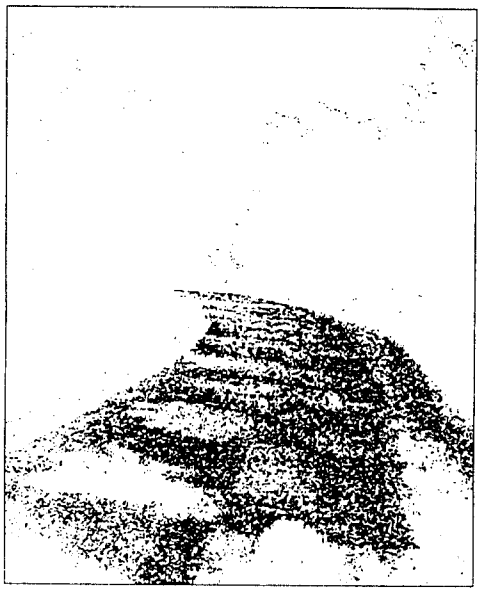

(a)

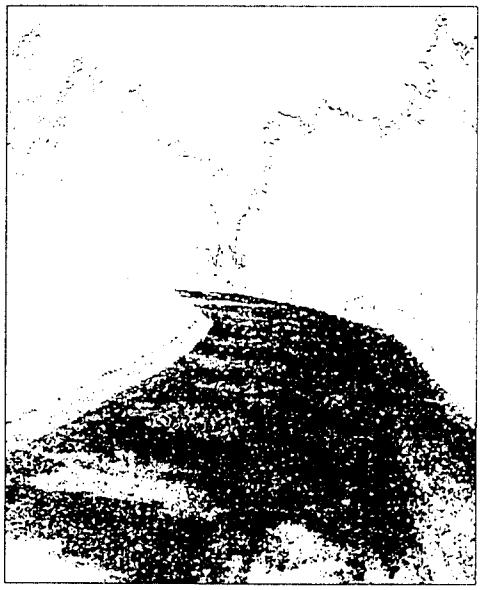

(b)

Fig. 3 Thresholded image at 50% level (a) and 90% level (b) using the proposed method.

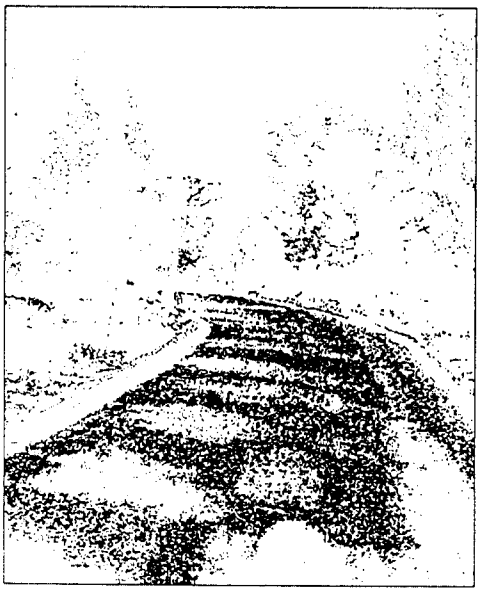

(a)

(b)

Fig. 4 Thresholded image at 50% level (a) and 90% level (b) without color normalization.

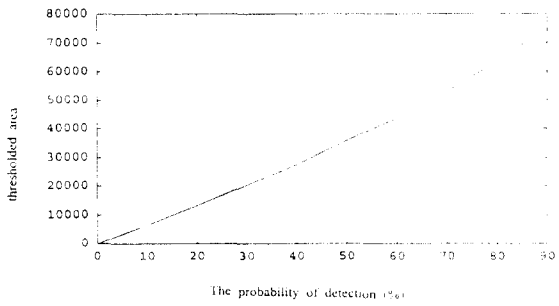

Fig. 5 The probability of detection vs. the area of the thresholded image.

Ⅳ. Conclusion

We chose normalized color in an effort to obtain the surface reflectance and reduce the influence of surface orientation and illumination component from the color image. Karhunen-Loeve transformation is applied to obtain principal components and found that normalized color components I3/I1 and I2/I1 are effective color features. We showed the relationship of the threshold value and the probability of false negative. From experiments, it was verified that the probability of detection is proportional to the area of thresholded region.

Ⅴ. Further Work

The performance of the segmentation will be improved with elaborate color constancy algorithms, calibration of image sensor and transfer function in the image aquisition process. Segmentation of the image in color parameter space has limitations. Postprocessing in image space can eliminate the noisy segmentation with small area.

Ⅵ. Acknowledgements

The author acknowledges the professor Thomas O. Binford from Stanford University for his helpful suggestions.

References

1. R. Ohlander, K. Price, and D.R. Reddy, "Picture Segmentation Using A Recursive Region Splitting Method," Computer Graphics and Image Processing, Vol. 8, No. 1, pp. 313-333, Aug. 1978.
2. Y. Ohta, T. Kanade, and T. Sakai, "Color Information for Region Segmentation," Computer Vision Graphics and Image Processing, Vol. 13, No. 1, pp. 222-241, May 1980.
3. C. Thorpe, S. Shafer, and T. Kanade, "Vision and Navigation for the Carnegie Mellon Navlab", Proceedings of Image Understanding Workshop, Los Angeles, California, pp. 143-152, Feb. 1987.
4. R. Bajcsy, L.S. Davis, M. Herman, and R. Nelson, "RSTA on the Move," Proceedings of Image Understanding Workshop, Monterey, California, pp. 435-456, Nov. 1994.
5. G. Healey and David Slater, "Global Color Constancy: Recognition of Objects by Use of Illumination-Invariant Properties of Color Distributions," Opt. Soc. Am. A, Vol. 11, No. 11, pp. 3003-3010, Nov. 1994.
6. J. Ho, B.V. Funt, and M.S. Drew, "Seperating a Color Signal into Illumination and Surface Reflectance Components: Theory and Applications," IEEE Transactions on Pattern Analysis and Machine Intelligence, Vol. 12, No. 10, pp. 966-977, Oct. 1990.
7. B.A. Wandell, "The Synthesis and Analysis of Color Images," IEEE Transactions on Pattern Analysis and Machine Intelligence, Vol. 9, No. 1, pp. 3-13, Jan. 1987.
8. M.J. Swain and D.H. Ballard, "Indexing via Color Histograms," Proceedings of IEEE ICCV, Osaka, Japan, pp. 390-393, Dec. 1990.
9. T. Uchiyama and M.A. Arbib, "Color Image Segmentation Using Competitive Learning," IEEE Transactions on Pattern Analysis and Machine In-

telligence, Vol. 16, No. 12, pp. 1197-1206, December 1994.
10. R.M. Haralick and L.G. Shapiro, Computer and Robot Vision, Addison-Wesley Publishing Company, Reading, Massachusetts, 1992.
11. F. Ennesser and G. Medioni, "Finding Waldo, or Focus of Attention Using Local Color Information," IEEE Transactions on Pattern Analysis and Machine Intelligence, Vol. 17, No. 8, pp. 805-809, Aug. 1995.
12. B.V. Funt and G.D. Finlayson, "Color Constant Color Indexing," IEEE Transactions on Pattern Analysis and Machine Intelligence, Vol. 17, No. 5, pp. 522-529, May 1995.
13. W.K. Pratt, Digital Image Processing, 2nd Ed., John Wiley and Sons, 1991.
14. S.U. Lee, S.Y. Chung, and R.-H. Park, "A Comparative Performance Study of Several Global Thresholding Techniques for Segmentation," Computer Vision, Graphics, and Image Processing, Vol. 52, No. 2, pp. 171-190, Nov. 1990.
15. Y.W. Lim and S.U. Lee, "On the Color Image Segmentation Algorithm based on the Thresholding and the Fuzzy c-Means Techniques," Pattern Recognition, Vol. 23, No. 9, pp. 935-952, Sep. 1990.
16. T.W. Anderson, An Introduction to Multivariate Statistical Analysis, 2nd Ed., John Wiley and Sons, Inc, 1984.
17. W.H. Press, B.P. Flannery, S.A. Teukolsky, and W.T. Vetterling, Numerical Recipies in C, Cambridge University Press, Cambridge, 1988.
18. R. Nevatia, "A Color Edge Detector and Its Use in Scene Segmentation," IEEE Transactions on System, Man, and Cybernetics, Vol. SMC-7, No. 11, pp. 820-826, Nov. 1977.

이 병 욱(Byung-Uk Lee) 정회원
1975년 3월~1979년 2월 : 서울대학교 전자공학과 학사
1979년 3월~1981년 8월 : 한국과학기술원 전기 및 전자공학과 석사
1985년 8월~1991년 6월 : Stanford University Electrical Eng. 박사
1981년 8월~1983년 4월 : 대한전선 Video개발부
1983년 5월~1985년 8월 : 대우전자 중앙연구소 Video개발부
1991년 7월~1995년 8월 : 대우전자 영상연구소 수석연구원
1995년 9월~현재 : 이화여자대학교 전자공학과 조교수